Article

Design and thermodynamic analysis of a hybrid gas turbine-steam methane reforming system

Minh Hoang Tran, Seyed Ehsan Hosseini*

Department of Mechanical Engineering, Arkansas Tech University, 1811 N Boulder Ave, Russellville, AR, 72801, USA

ARTICLE INFO	ABSTRACT
	This study proposed and evaluated the new hydrogen production design of the Gas Turbine - Steam Methane Reforming (GT-SMR) hybrid process. The superheated byproduct gas from the GT system is utilized as a combustion agent for the boiler of the SMR system, minimizing the required heat energy input for hydrogen production. The overall energy consumption and energy generation are calculated and simulated to determine the system's operational performance. Under no efficiency losses, the design is tested to understand how the significant input parameters such as temperature, pressure, and steam/methane ratio (S/C) affect the system's overall performance. From the data generated, the system's efficiency was directly proportional to the pressure and temperature while inversely proportional to the S/C values. However, in actual applications, the menthane conversion rate often fluctuated depending on the adjustments of these factors, regardless of their thermodynamic relationship with the SMR efficiency. With the addition of other energy waste information, a complete simulation showed the reversed effect of pressure. Although the temperature and S/C ratio improved the overall performance, the hybrid system efficiency reached its limits beyond certain values.

1. Introduction

Hydrogen gas has become more popular as a discussion topic in recent decades as it holds a vital position in sustaining the current oil and agricultural industry as well as determining the future's energy path. Hydrogen has the lowest molecule weight and a high energy-to-weight ratio compared to traditional fuel. This makes hydrogen an attractive alternative to power transportation to reduce the CO_2 emission from combustion engines. Other than fuel cells and the potential replacement of fossil fuels, hydrogen has been widely utilized in major industrial applications. Nearly 70% of produced hydrogen in the United States is used in the petroleum refining industry [1]. Another 20% is utilized in producing fertilizer for agricultural usage. Despite its critical role in industry, hydrogen production is not a simple task due to constraints in production and exploitation methods. To generate hydrogen gas, reactions are usually required to be endothermic, leading to more energy input to sustain the conversion than the possible extracted energy of hydrogen. This limits hydrogen production to a few industries with abundant or pre-existing heat sources to provide the necessary reaction energy. Currently, only a few hydrogen-generating methods are widely used. Proton Exchange Membrane Electrolysis Cell (PEMEC) uses electricity to ionize

the water particles and separate them into pure hydrogen and oxygen gas. It uses solid polysulfonated membranes as both a separator and a gateway for ions without needing electrolytes. Due to its electricity dependence, PEM efficiency can vary between 50% and 70%, while a study has shown a possibility of 94% is achievable [2]. Despite its high efficiency, the PEMEC structure requires the usage of noble metals like Platinum, Iridium, and Ruthenium. Currently, Platinum material is considered the state-of-the-art electrocatalyst for the PEM cathode [3]. As these materials are rare and precious metals, the cost of the PEM electrolyzer is unattractive for mass-scale hydrogen production. Its lifespan is also a major concern, with durability at around 30,000h to 40,000h [4]. Another method that can harness the pre-existing heat sources is Solid Oxide Steam Electrolysis (SOSE). Although SOSE still essentially relies on electricity, it uses higher temperatures (600-900℃) to convert water to hydrogen gas. This high-temperature input usually comes from thermal energy utilization from power plants or boilers. Its efficiency can be higher through optimization than other conventional room-temperature hydrogen production methods [5]. Despite its benefits, the SOSE investment cost is relatively high due to its usage of heat-resistant ceramic electrolytes and other materials [6].

Nomenclature

E	molar exergy
E_{chem}	chemical exergy
E_{mix}	mixture exergy
E_{phys}	physical exergy
E_Q	heat transfer exergy
E_W	physical exergy
ε	efficiency
h	enthalpy
m	mass
n	molar number
Q	heat transfer energy
R	universal gas constant
S	entropy
T	temperature
W	work energy
x_i	mole fraction

While its efficiency is competitive, extreme temperatures accelerate the degradation rate of its electrolyte, reducing its overall lifespan [7]. The SOSE technology is also immature and less commercially proven than other high-temperature hydrogen production methods. Today, most hydrogen is extracted from natural gas through Steam Methane Reforming (SMR). The process involves mixing natural gas with hot steam, including the catalyst in the reformer, to create an endothermic chemical reaction. The reaction generates a mixture of hydrogen, carbon monoxide, and CO_2 [8]. After that, the carbon monoxide is transferred through a water-gas shift (WGS) system to react with steam and generate additional hydrogen and CO_2 gas. However, this hydrogen is impure and unusable since it contains other gases. Therefore, the mixture goes through pressure swing absorption (PSA) to remove impurities and separate pure hydrogen [9]. All the CO_2 can then be captured and loaded into storage or trapped underground to reduce the emission to the atmosphere. SMR is currently the most common production method, accounting for 98% of all hydrogen production [10]. For SMR to operate correctly, it demands a very high heat energy source. During running, the temperature of the reformer in the SMR can reach anywhere from 700℃ to 1000ºC [11-13]. A large amount of input fuel is compulsory to elevate the steam and methane temperature to this optimal condition. On average, up to 35% of the energy input is wasted during the SMR operation [14]. This waste contributes to excess CO_2 emissions that cannot be utilized and is deemed counterproductive in reducing greenhouse gases.

Acknowledging this limitation, multiple SMR designs have been incorporated into other energy systems to utilize the already available heat source. One such design is a proposal to exploit the steelmaking waste heat in steel production to bring the temperature of SMR's fuels to the optimal point [15]. In this model, the exergy loss was evaluated at 65.8%, most of which was at the heating furnace (59.5%). Multiple factors can contribute to the common low exergy efficiency of the SMR system. Besides the temperature problem, in real-life operation, the process is also affected by the system pressure, the efficiency of the system's components, the reaction rate, the undesired chemical presence, etc. All these contributors make the hydrogen production method relatively unpredictable. Difference testing conditions under different research with different calculation methods produce different outcomes with exergetic efficiency varying from 59% to 95% [16-18].

2. System design and modeling

For this paper, the SMR system is proposed to be incorporated into a gas turbine system (GT-SMR). The exiting superheated air from the gas turbines can react with methane gas in the flameless boiler to generate the necessary heat to sustain the SMR process. This paper analyzed the exergetic feasibility of the SMR system based on various conditions. It generated the simulating model to test the effect of multiple factors on the model based on the data provided by other academic sources. The SMR thermodynamic process is illustrated in Figure 1. The full process is divided into two separate processes: the gas turbine and the SMR process. Air is compressed and heated in the combustion chamber in the gas turbine process. The superheated air flows into the gas turbine to supply the desired energy to generate electrical power. This flow replicates the ordinary gas turbine system. At this point, the post-turbine air temperature is around 400-600℃ [19]. The hot air is then fed into a flameless combustion boiler in the SMR system, which is auto-ignited when mixed with methane gas. The amount of available oxygen is low at the step as it has been utilized in the gas turbine's combustion chamber. However, the required oxygen to sustain the flameless combustion mode can be as low as 3% concentration [20]. This allows the SMR flameless boiler to operate efficiently without additional air supply. Methane automatically combusts with the gas turbine exhaust gases when the temperature reaches 540℃ [21]. The flameless combustion boiler is used to heat water and make steam for the SMR system. The gas turbine capacity for this individual system is estimated to range between 8MW and 17 MW, depending on the ratio of steam and methane (S/C) and output temperature. For the SMR system to operate, water is supplied through the pipeline with normal pressure at step 7, while methane is directed under high pressure at step 5. Methane gas is transported in the industrial pipeline under a high pressure of 10 MPa; therefore, no pumps are required before running the combustion chamber in the SMR system [22]. In contrast, water pressure is generally lower and requires a pump to increase the pressure to the same as the pressure with methane (step 8). Both methane and water run through the combustion chamber to heat up to the minimum temperature of 700 ℃ at steps 6 and 9. The hot methane gas and steam enter the SMR system where steam methane reaction occurs. The SMR and WGS are combined into one reformer step between steps 6,9 and 10. The products after the reformer are hydrogen gas and carbon dioxide.

2.1 Exergy and related performance analysis

The steam methane chemical reaction in the reformer is as follows:

$$CH_4 + 2H_2O \rightarrow CO_2 + 4H_2 \tag{1}$$

To evaluate the efficiency of the SMR system, exergy values are determined for both reactant and product. All potential energy used during a thermodynamic process is quantified under exergy. Exergy values present both the maximum obtained work in a system and the loss of potential work due to irreversibility. In a typical thermodynamic system, total exergy E_Σ includes all heat transfer exergy E_Q, work exergy E_W, physical exergy E_{phys}, chemical exergy E_{chem}, and mixture exergy E_{mix} [23].
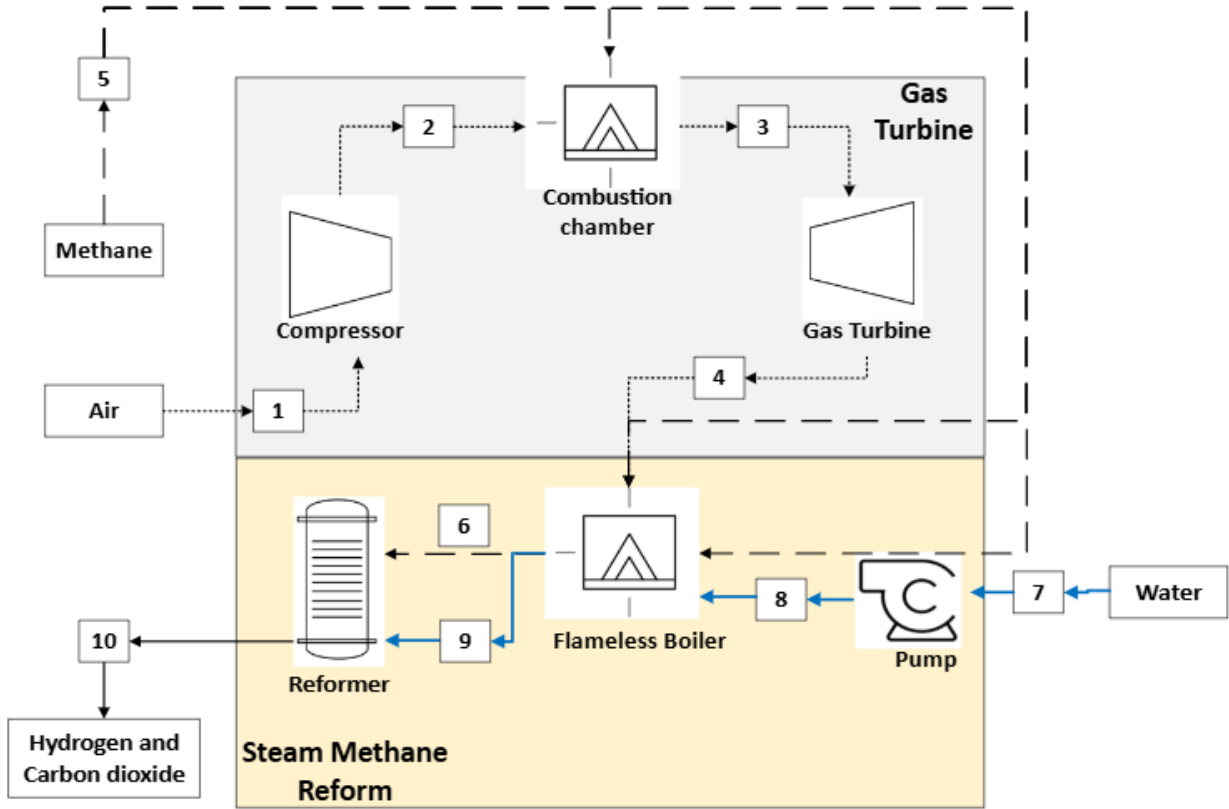
Figure 1. Combined gas turbine and SMR system thermodynamic process

$$E_{\Sigma} = E_Q + E_W + E_{phys} + E_{chem} + E_{mix} \qquad (2)$$

The general heat transfer exergy is given by:

$$E_Q = Q\left(1 - \frac{T_0}{T}\right) \qquad (3)$$

where T_0 is the reference temperature, T is the temperature at which the heat transfer occurs, and Q is the heat transfer [24].

For this design, work exergy is the output work performed by pumps, turbines, or engines in a fully controlled volume. General work exergy is extracted from the change in total enthalpy between the inlet and outlet [24].

$$E_W = W_{cv} = m(h_i - h_o) \qquad (4)$$

Where m is the mass of the material flowing through the apparatus, h_i is the inlet enthalpy of the material flow, and h_o is the outlet enthalpy of the material flow.

During the process, the physical exergy of both products and reactants is present as both the temperature and pressure change regarding the environment [23]. During movement across the system, substances' states change depending on the pressure and temperature difference between their initial and final states. This generates work, which is termed physical exergy. This exergy represents all potential energy generated besides the actual utilized work from turbines and engines.

$$E_{phys} = m[\,(h - h_o) - T_0(s - s_0)] \qquad (5)$$

For the chemical reaction in the reformer, the chemical exergy is determined as:

$$E_{chem} = m \sum_i^n n_i e_i \qquad (6)$$

where e_i is the molar exergy of that substance at the reference temperature, n_i is the mole number of the substance in the reaction [25, 26].

Unlike physical exergy, which can only account for the physical change, chemical exergy utilizes the Gibbs formation energy to account for the released or absorbed energy during chemical reactions. As the product gas H_2 and CO_2 from the reformer is discharged as a mixture, entropy increases, and irreversibility is introduced into the system. Mixture exergy accounts for this irreversibility at the outlet of the reformer [27]. The mixture exergy depends directly on the mole proportion of each chemical in the mixture.

$$E_{mix} = T_0 R \sum_i^n n_i x_i \ln(x_i) \qquad (7)$$

where T_0 is the reference temperature, R is the universal gas constant, n_i is the mole number of component i, and x_i is the mole fraction of component i in the mixture.

The exergy efficiency of the system is extracted as the ratio of total output exergy $E_{\Sigma, product}$ over total input exergy $E_{\Sigma, reactant}$ [23].

$$\varepsilon = \frac{E_{\Sigma, product}}{E_{\Sigma, reactant}} = \frac{\sum_i^{n, product} E_i}{\sum_i^{n, reactant} E_i} \qquad (8)$$

where E_i includes E_Q, E_W, E_{phys}, E_{chem}, and E_{mix}

For the SMR system, hydrogen production exergy efficiency can also be calculated based on only the output exergy of hydrogen alone to have more accurate results and exclude the effects of other byproduct gases.

$$\varepsilon = \frac{E_{\Sigma, hydrogen}}{E_{\Sigma, reactant}} = \frac{\sum_i^{n, hydrogen} E_i}{\sum_i^{n, reactant} E_i} \qquad (9)$$

ε value ranges from 0 to 1 as the total output exergy cannot surpass the total input energy.

For $E_{\Sigma, product} > E_{\Sigma, reactant}$, the system requires more input energy than the current designed model.

2.2 Simulation of the SMR system under perfect condition

A simulation of the SMR system was performed to determine the feasibility of the process and analyze the optimal conditions for the system. For the methane at step 5 and the water at step 7, their temperature was chosen to be 25℃ while the water's pressure was set at 0.277 MPa. A simulation of different conditions was performed to observe how all factors affect the overall SMR system performance under various conditions. A predicted model was also created to show how well the data (in case of variance) fits within the model. For the perfect condition, the exergy efficiency was based on the total output of all products of the SMR system to understand the system's capability. The simulation steps were completed as follows:

- The combustion chamber temperature provided the minimum temperature of the SMR process of 700 ℃ and the pressure was maintained at 0.5MPa (the same pressure as the provided methane in the pipeline). The total exergy of reactants and products was calculated to extract the overall exergy efficiency of the system under the perfection ratio and the reaction of steam and methane.
- The ratio of steam and methane (S/C) was increased from 2:1 to 3.5:1 to reduce the risk of carbon deposition on the catalyst surface [28]. In this circumstance, the overall exergy efficiency of the system was tested.
- The flameless combustion chamber temperature was raised to 1,100℃. This exceeded the limit of the temperature of conventional SMR of 1000℃ to determine the effect of temperature on the total exergy of reactants and products and their efficiency [13].
- The system pressure was raised to 2.5 MPa to observe the impact of the pressure on the system's efficiency.
- Different temperatures and pressures were tested and analyzed to determine the system's most important key factor and the best dual values.

2.3 Simulation with efficiency waste and unreacted materials

Several uncontrollable factors directly affect the system's exergy efficiency during actual operations. These factors increase the exergy waste during operation, causing less energy to convert reactants to hydrogen gas. These factors can be related to heat loss, pressure loss, unreacted materials, factorial effects of input conditions, etc. One of the major contributors to exergy waste is boiler efficiency. Different furnace and burner designs affect the overall efficiency of the boilers. Their performance also depends on the quality of the combustion and the type of fuel used. For example, if the combustion reaction is incomplete, carbon monoxide is produced, and its presence reduces the boilers' performance [29]. Unused or unwanted heat transfer due to inadequate insulation can also lower the efficiency values. For a large-scale gas-fired steam boiler, the efficiency of the boiler

η_{boiler} is considered 83.0% [30]. Pump efficiency is another contributor to exergy waste. The pump controls water pressure and flow rate in the SMR system. When the fluid moves through pipes and values, the friction between the fluid and the pump's component is generated, causing a reduction in pump efficiency. As the rate of flow increases, the overall pump efficiency increases. However, when the flow rate reaches a certain limit, the flow transforms from laminar flow to turbulence flow, leading to degradation in overall efficiency [31]. Overall, the water pump efficiency can be 82-87% [32]. Gas compressor performance is also vital in exergy efficiency simulation since the methane gas needs to have a pressure equilibrium with the steam in the SMR chamber. Similarly, the efficiency of methane compressors can be found to be at almost the same value range [33].

To achieve maximum hydrogen production, the whole methane gas must react with hot steam in the SMR chamber. Although the S/C ratio is usually considered above 2, a fraction of methane remains untouched, which can be traced back to catalyst degradation over time, for which the methane conversion ability is directly affected. Other conditions, such as high pressure, also have been observed to negatively affect the methane conversion of catalyst [34]. Park et al. [33] tested and measured the methane conversion rate under different temperatures, pressures, and S/C ratios in the SMR system [35]. Their collected data was reconstructed and modeled, as shown in Figure 2. The conditions were tested during the experiment with co-affecting factors set at fixed points. For the effect of temperature on the methane conversion, the pressure was set at 1MPa and an S/C ratio of 3 (Figure 2a). The temperature was then adjusted to be at 830℃ with pressure at 1MPa to generate the methane conversion data with respect to the S/C ratio change (Figure 2b). Figure 2c shows the methane conversion efficiency according to the pressure variation with the temperature at 830℃, and S/C ratio of 3. A general empirical equation for methane conversion was generated:

$$\eta_{CH_4\ Conv} = -0.1048 + 0.00128T_{boiler} - 5.91 * 10^{-6}(T_{boiler} - 822.11)2 + 0.04396R - 0.02428(R - 2.97)^2 - 1.56 * 10^{-4}P_{pump} - 8.917 * 10^{-8}(P_{pump} - 1052.78)^2 \qquad (10)$$

Where R is the S/C ratio, T_{boiler} is the output temperature of the methane and steam boiler, and P_{pump} is the output pressure of the water pump. Using the model, the estimation of unreacted methane amount can be determined for application.

The final simulation fully incorporated the efficiency coefficients of boiler, pumps, and compressors as well as the actual data of methane conversion in the SMR chamber to generate the most suitable model for SMR exergy calculation. The model was then tested with the results of different papers to compare the efficiency deviation. For this simulation, the exergy efficiency was based on the output exergy of only hydrogen of the SMR system for more accurate values.

3. Results and discussion

3.1 Perfect condition with no loss

For the preset condition, the total input exergy $E_{\Sigma, reactant}$ was 64.64MW, and the total output exergy $E_{\Sigma, product}$ was 63.08MW for 1 kg of methane. Exergy loss was calculated at 1.56MW, and the system's efficiency was considered to be 97.57%. All the exergy data has been shown in Table 1. Table 1 also shows how each exergy type contributes to the total exergy, with chemical exergy having the highest percentage.
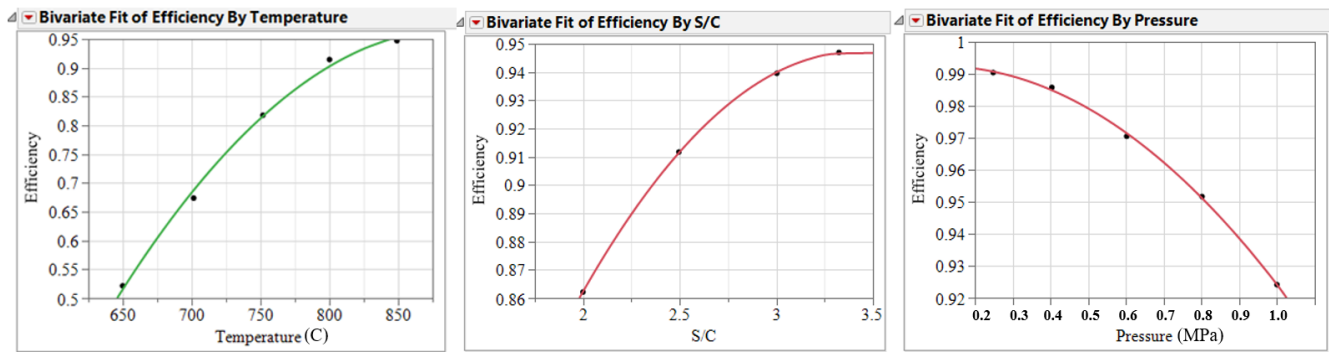
Figure 2. (a) Methane consumption efficiency according to temperature; (b) Methane consumption efficiency according to S/C ratio; (c) Methane consumption efficiency according to pressure

Table 1. Exergy type and their contribution to the overall input and output of the system

Exergy	Step	Value (MW)	% of Input/ output
Heat transfer exergy at the combustion chamber	6,9	7.55	11.68
Work exergy at water pump	8	$-503 * 10^{-4}$	0.08
Physical exergy of reactant	6.9	4.5	6.96
Chemical exergy of reactant	6.9	52.6	81.37
Physical exergy of product	10	4.58	7.26 (of output)
Chemical exergy of product (including mixture exergy)	10	58.49	92.74 (of output)
Total input exergy		64.64	100
Total output exergy		63.09	97.57

This can be traced back to the high chemical exergy of methane due to its energy content (824,350 kJ/kmol) and the potential to undergo a reforming reaction. In addition, the product gas of H_2 also has considerable chemical exergy (235,250 kJ/kmol) since it is an energy-dense fuel. Almost 90% of initial exergy is retained in the chemical bonds of the products, particularly H_2. Figure 3 shows the potential amount of hydrogen produced by the gas turbine capacity. This is based on the simple gas turbine efficiency of 35% [36]. As the gas turbine capacity increases, the potential amount of the produced hydrogen increases. As the S/C increases from 2 to 3.5, the efficiency of the overall SMR system decreases from 97.57% to 90.71%, as demonstrated in Figure 4. The hike in steam ensured there was no unreacted methane in the output of the SMR system and reduced the risk of carbon deposition. However, this also means the system requires more heat transfer exergy in the combustion chamber and work exergy in the water pump to produce the same amount of hydrogen. It also introduced the presence of excess steam in the output mixture, causing a decrease in overall efficiency. For the temperature effect, the overall efficiency decreased as temperature increased from 700℃. When the temperature reached 1100℃, the overall efficiency was reduced to 92.28% (Figure 5a). Based on the exergy equations, only the heat transfer exergy and physical exergy were affected during the temperature change. The input thermal-dependent exergy included both heat transfer exergy at the combustion chamber and the physical exergy of the reactant, while the output thermal-dependent exergy only contained the physical exergy of the product. When the temperature surpassed the lower limit, the exergy difference between the product and reactant increased from 7MW to 11.44MW (a 53.4% increase) at 1100℃ in Figure 5b. It can be stated that, based on the data, the temperature is inversely proportional to the efficiency of the system.
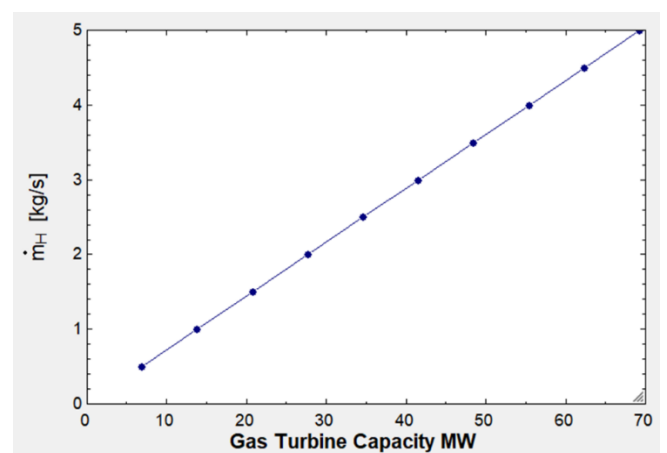
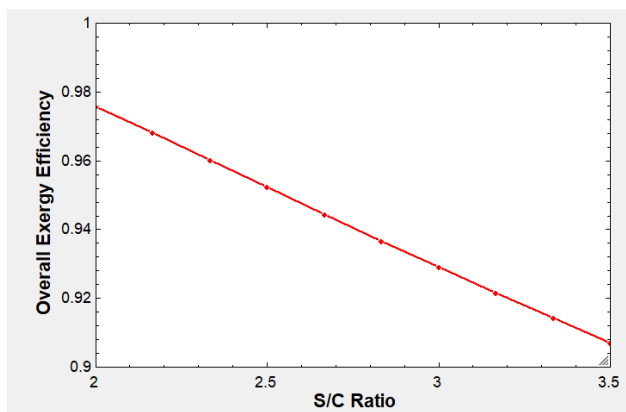**Figure 3.** Gas turbine capacity vs. potential production mass of hydrogen gas

Figure 4. Effect of s/c ratio on the system's overall exergy efficiency under perfect condition

The lower temperature limit was found to be 550℃. On the other hand, pressure had a positive impact on the exergy efficiency of the system. When the pressure increased from 0.5MPa to 2.5MPa, efficiency increased from 97.57% to 98.4% as shown in Figure 6a. Pressure change affects both the physical exergy of chemicals and the work exergy at the water pump. As the contribution of the work exergy at the water pump (and hypothetical methane pump) is neglectable, the physical exergy of the reactants and products were compared to each other in Figure 6b. Since more pressure was added to the system, the physical exergy of the product expanded faster than the reactant, leading to an efficiency increase. Due to hydrogen's low molecular weight and higher specific energy content, it tends to expand more under high pressure, which is why its physical exergy grows faster. This results in the higher physical exergy of the product. To overcome the high physical exergy of the product, a large amount of heat transfer exergy is needed.

All data fit well, with 99.92% of the variance in the response variable explained by the model. When cross-testing, the data showed the performance of the system was significantly affected by the ratio S/C. The temperature also has a big impact on the system, while the pressure has the least effect. The maximum efficiency was achieved at 98.5% under the ratio S/C=2, the combustion temperature at 700℃, and the pressure of 2.5MPa.
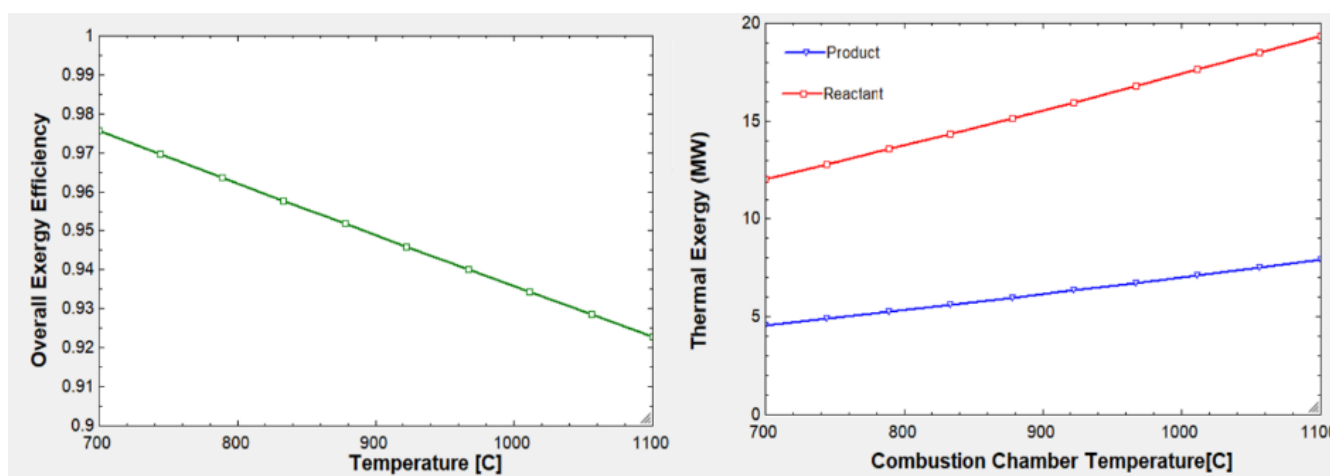
Figure 7 illustrates the testing of the different conditions, with the shade representing ≥90% efficiency zone (total output of all products). Based on the results, some key points can be gathered and shown in Figure 7:
- At the ratio S/C=2, the exergy efficiency was maintained at ≥ 90% under all combustion temperatures and pressure levels (Figure 7a).
- At the ratio S/C=3, for ε ≥ 90%, the maximum temperature was 960℃ at the maximum pressure of 2.5MPa (Figure 7c).
- At the minimum pressure of 0.5MPa (the least work for pump), the maximum S/C ratio was 2.7 at 1000℃ (See Figure 8d). At the maximum pressure of 2.5MPa (the most work for pump), the maximum S/C ratio was 2.8 (Figure 7f).
- Under all S/C values and pressure levels, the exergy efficiency was also maintained at ≥ 90% at the temperature of 700℃ to 850℃ (Figure 7g and 7h).

3.2 Simulation with waste and unreacted materials

After accounting for all the waste and unreacted materials, the model generated results, as shown in Figure 8. The shaded area represented ≥70% exergy efficiency of the system (only hydrogen) after applying for the loss. Some observations can be made:
- The S/C change has small positive effects on the combination of temperature and pressure for ≥70% exergy efficiency. As the S/C ratio passed over 2.5, its effect is negligible, as shown in Figure 8c. Referring back to Figure b, the efficiency positive slope decreases gradually as the S/C ratio keeps increasing. However, increasing excess steam causes an increase in exergy waste, hence leading to the reverse efficiency trend.
- Pressure had a negative effect overall on the system. As pressure increased from 0.5 MPa to 1.5 MPa, the ≥70% exergy efficiency was confounded within the minimum and maximum temperature range between 840 ℃ and 990 ℃ for the S/C ratio between 2.5 and 2.8 in Figure 8e. As pressure increased to 2.5MPa, no plausible scenarios achieved ≥70% exergy. Previously, the pressure had a small positive effect on the overall system. However, when there is both the presence of excess methane and steam, the increase in pressure might inhibit the endothermic reaction in the SMR system while increasing the input exergy of the system.

Figure 5. (a) Effect of temperature on the system's overall exergy efficiency under perfect condition, (b) Thermal exergy of products and reactants over temperature range
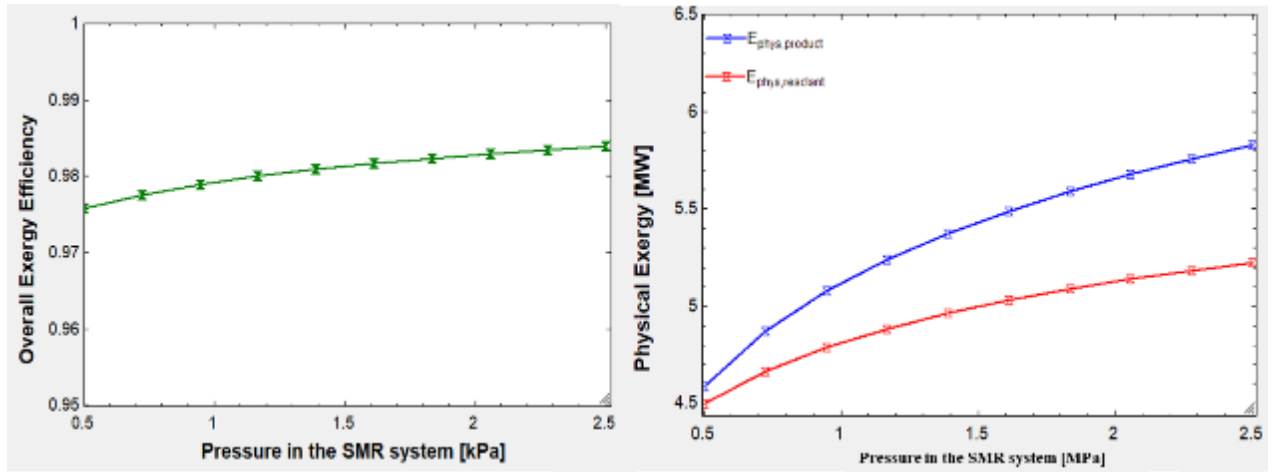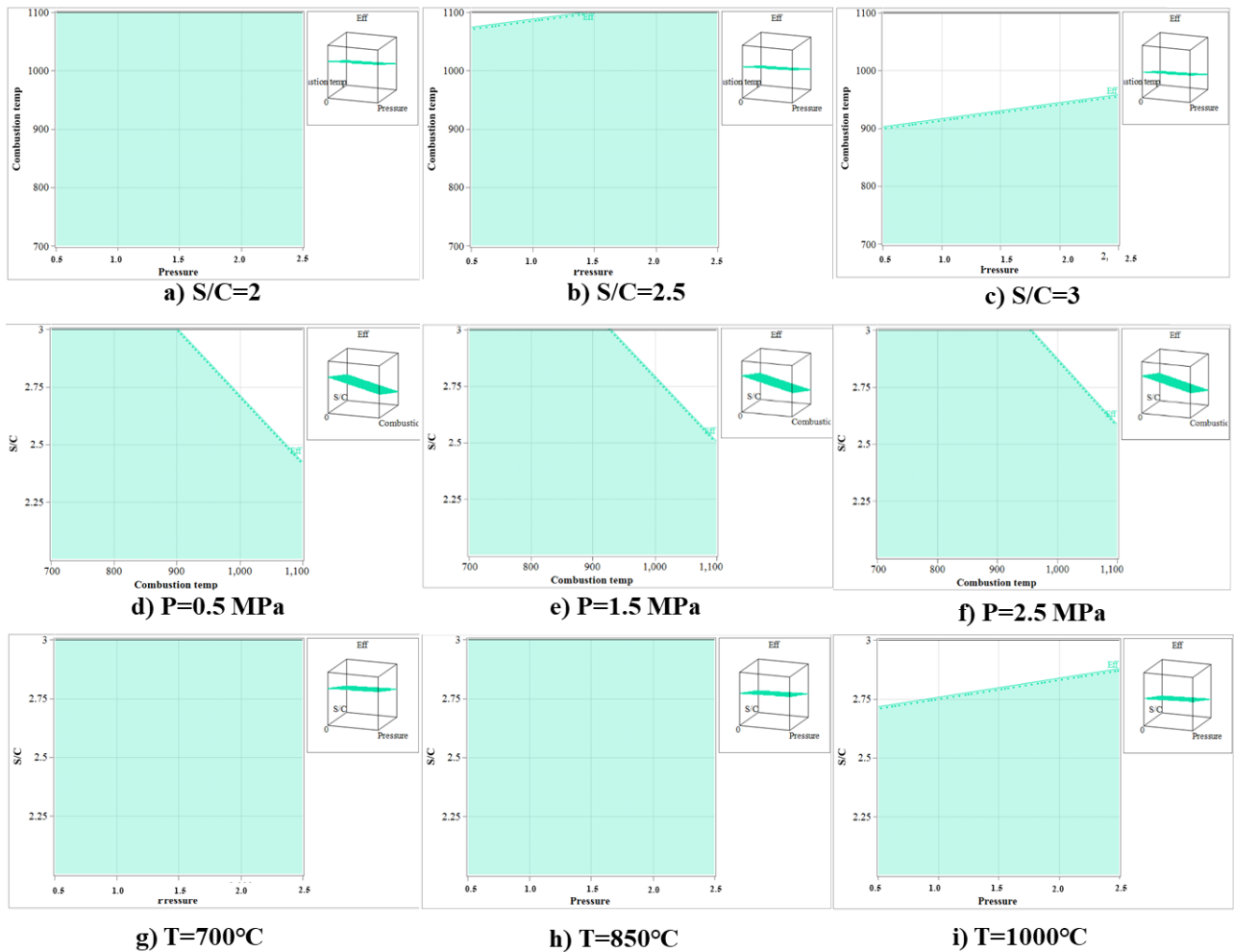
Figure 6. (a) Effect of pressure on the system's overall exergy efficiency under perfect condition, (b) physical exergy of products and reactants over the temperature range

Figure 7. (a-c) 90% exergy efficiency area on the pressure and temperature graph under different S/C ratio, (d-f) 90% exergy efficiency area on S/C and temperature graph under different pressures, (g-h) 90% exergy efficiency area on S/C and pressure graph under different temperatures
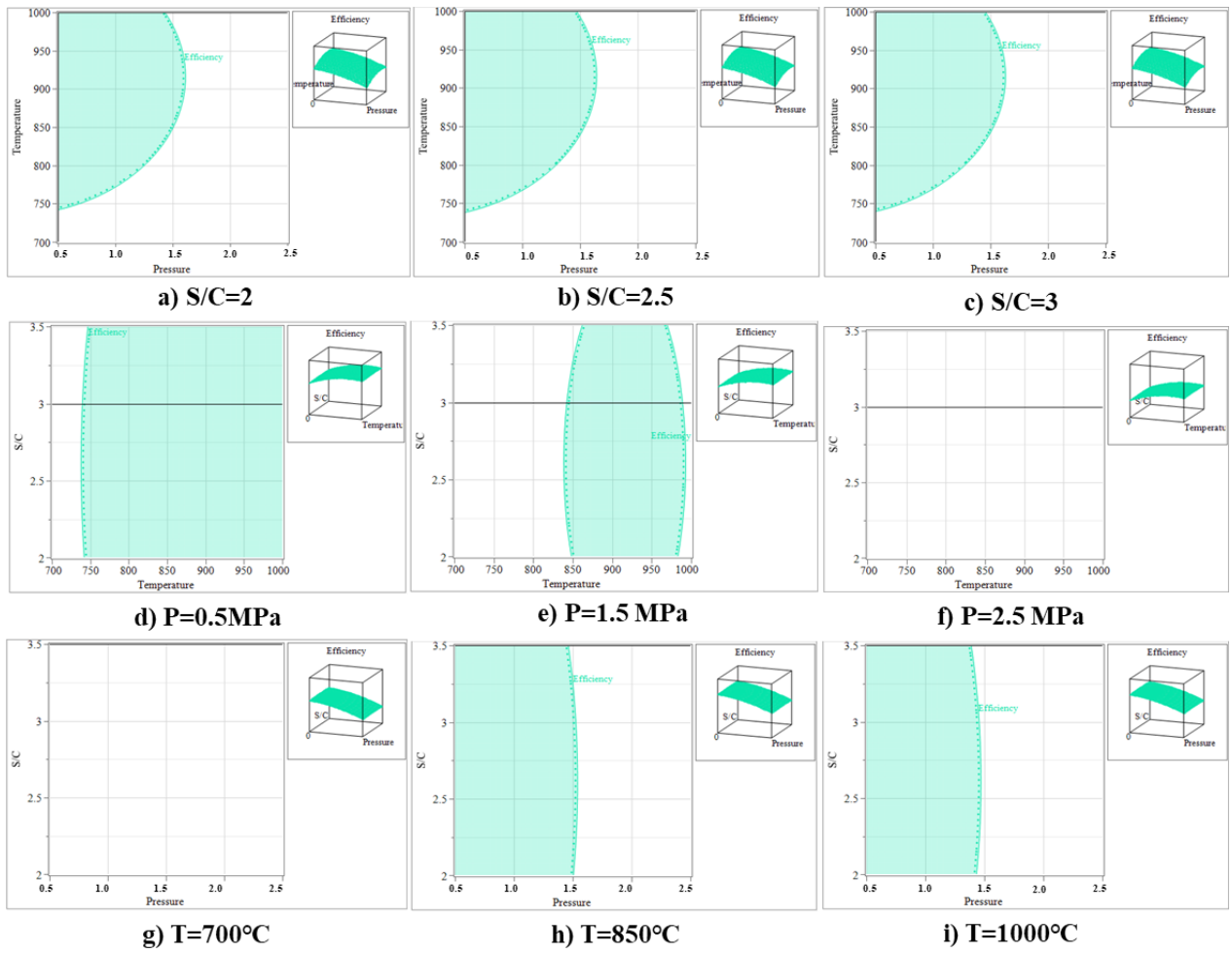
Figure 8. (a-c) 70% exergy efficiency area on the pressure and temperature graph under different S/C ratio, (d-f) 70% exergy efficiency area on S/C and temperature graph under different pressures, (g-h) 70% exergy efficiency area on S/C and pressure graph under different temperatures

Table 2. Exergy efficiency comparison with different sources under various conditions

T (℃)	P (MPa)	S/C	η_{boiler}	η_{pump}	Referred Exergy Efficiency	Calculated Exergy Efficiency	Note	Reference
700	1	3.2	0.9	0.85	62.7%	59.4%	Only hydrogen in the output exergy value	[38]
850	3.5	2.5	NA	NA	88.7%	82.9%	Total output exergy value	[16]
700	1	3	NA	NA	94.6%	93.7%	Total output exergy value, excluding HX and PEMFC	[17]
400	1	NA	NA	NA	94.3%	90.8%	Total output exergy value, exclude heat exchanger, cooling system	[37]
900	3.5	NA	NA	NA	78.5%	83.8%	Total output exergy value	[39]
925	2.5	3.26	NA	NA	79.9%	88%	Total output exergy value	[40]

* The exergy efficiency at the lowest temperature value of 550℃

- In general, increasing temperature has a positive effect on exergy efficiency. Figure 8g showed that the exergy waste was too high and reduced the overall exergy efficiency below the 70% exergy efficiency rate at the temperature of 700 ℃. As the temperature was raised to 850 ℃The efficiency limit can be achieved and surpassed for pressure below 1.6 MPa, as shown in Figure 8h. As the temperature passes 990 ℃, the overall exergy efficiency decreased.
- The model showed a maximum efficiency of 86.4% at the condition of S/C ratio at 2.6, pressure at 0.5 MPa, and temperature of 900℃.

The model was then compared with six different studies to see how well it correlated with actual data. Table 2 shows the different conditions in temperatures, pressures, and S/C ratio as well as the calculated exergy efficiency and the referred values. Overall, the model correlated well with the difference within the 10% variation. The only exemption was the value from the exergy analysis paper of Hajjaji et al. [37], where the temperature was 400℃. The model's lowest temperature limit was 550℃. When applying this limit to the model, the calculated exergy efficiency is comparable to the referred value.

4. Conclusion

This work proposed an SMR system incorporated with a gas turbine system and generated a simulation model for the SMR system that can be utilized to calculate performance efficiency. Some conclusions can be made as follows:

- Based on the output superheated gas from the gas turbine system, a flameless boiler can be designed to produce heat energy for the SMR system with an absolute exergy efficiency of 97.57% with no loss, and at perfect condition of S/C ratio of 2, temperature of 700℃, and pressure of 0.5 MPa.
- For absolute boiler and pump efficiency and no variation in methane conversion in the SMR chamber, the S/C ratio and temperature have a negative effect on the exergy efficiency, while pressure has a positive impact on the exergy efficiency.
- As methane conversion efficiency in the SMR chamber is directly affected by pressure, S/C ratio, and temperature, the pressure increase reduces the exergy efficiency while the S/C ratio and temperature increase promote exergy efficiency.
- For the simulation model, the best condition was proposed when the S/C ratio at 2.6, pressure at 0.5 MPa, and temperature of 900℃ to produce a hydrogen exergy efficiency of 86.4%.

Ethical issue

The authors are aware of and comply with best practices in publication ethics, specifically with regard to authorship (avoidance of guest authorship), dual submission, manipulation of figures, competing interests, and compliance with policies on research ethics. The authors adhere to publication requirements that the submitted work is original and has not been published elsewhere.

Data availability statement

Datasets analyzed during the current study are available and can be given following a reasonable request from the corresponding author.

Conflict of interest

The authors declare no potential conflict of interest.

References

[1] Hosseini, Seyed Ehsan, Hydrogen Diplomacy. Future Publishing LLC, 2024. DOI: https://doi.org/10.55670/fpll.book/1, ISBN: 979-8-9906790-0-9

[2] K. A. Lewinski, D. van der Vliet, and S. M. Luopa, "NSTF Advances for PEM Electrolysis - the Effect of Alloying on Activity of NSTF Electrolyzer Catalysts and Performance of NSTF Based PEM Electrolyzers," ECS Trans, vol. 69, no. 17, pp. 893–917, Sep. 2015, doi: 10.1149/06917.0893ecst.

[3] T. Wang, X. Cao, and L. Jiao, "PEM water electrolysis for hydrogen production: fundamentals, advances, and prospects," Carbon Neutrality, vol. 1, no. 1, p. 21, Dec. 2022, doi: 10.1007/s43979-022-00022-8.

[4] A. Z. Tomić, I. Pivac, and F. Barbir, "A review of testing procedures for proton exchange membrane electrolyzer degradation," J Power Sources, vol. 557, p. 232569, Feb. 2023, doi: 10.1016/j.jpowsour.2022.232569.

[5] D. Elrhoul, M. Naveiro, and M. Romero Gómez, "Thermo-Economic Comparison between Three Different Electrolysis Technologies Powered by a Conventional Organic Rankine Cycle for the Green Hydrogen Production Onboard Liquefied Natural Gas Carriers," J Mar Sci Eng, vol. 12, no. 8, p. 1287, Jul. 2024, doi: 10.3390/jmse12081287.

[6] L. Mingyi, Y. Bo, X. Jingming, and C. Jing, "Thermodynamic analysis of the efficiency of high-temperature steam electrolysis system for hydrogen production," J Power Sources, vol. 177, no. 2, pp. 493–499, Mar. 2008, doi: 10.1016/j.jpowsour.2007.11.019.

[7] Q. Ma et al., "Electrochemical Performances of a Solid Oxide Electrolysis Short Stack Under Multiple Steady-State and Cycling Operating Conditions," Inorganics (Basel), vol. 12, no. 11, p. 288, Nov. 2024, doi: 10.3390/inorganics12110288.

[8] Locke, Karyssa. "The urgency of hydrogen: environmental issues and the need for change." Future Sustainability 2.2 (2024): 46-58. https://doi.org/10.55670/fpll.fusus.2.2.5

[9] Chowdhury, MD Farhan Imtiaz, MD Fahim Sadat Bari, Muhaiminul Islam, Wasif Sadman Tanim, and Redoy Masum Meraz. "Unlocking the potential of green hydrogen for a sustainable energy future: a review of production methods and challenges." Future Energy (2024): 18-46. https://doi.org/10.55670/fpll.fuen.3.4.2

[10] Noor, Wahid Bin, and Tanvir Amin. "Towards sustainable energy: a comprehensive review on hydrogen integration in renewable energy systems",Future Energy3(4), 1-17. DOI: https://doi.org/10.55670/fpll.fuen.3.4.1

[11] J. Wang, Z. Liu, C. Ji, and L. Liu, "Heat Transfer and Reaction Characteristics of Steam Methane Reforming in a Novel Composite Packed Bed Microreactor for Distributed Hydrogen Production," Energies (Basel), vol. 16, no. 11, p. 4347, May 2023, doi: 10.3390/en16114347.

[12] T. Pröll and A. Lyngfelt, "Steam Methane Reforming with Chemical-Looping Combustion: Scaling of

Fluidized-Bed-Heated Reformer Tubes," Energy & Fuels, vol. 36, no. 17, pp. 9502–9512, Sep. 2022, doi: 10.1021/acs.energyfuels.2c01086.

[13] "Hydrogen Production: Natural Gas Reforming," Office of Energy Efficiency & Renewable Energy. Accessed: Oct. 20, 2024. [Online]. Available: https://www.energy.gov/eere/fuelcells/hydrogen-production-natural-gas-reforming

[14] F. J. Durán, F. Dorado, and L. Sanchez-Silva, "Exergetic and Economic Improvement for a Steam Methane-Reforming Industrial Plant: Simulation Tool," Energies (Basel), vol. 13, no. 15, p. 3807, Jul. 2020, doi: 10.3390/en13153807.

[15] N. MARUOKA, H. PURWANTO, and T. AKIYAMA, "Exergy Analysis of Methane Steam Reformer Utilizing Steelmaking Waste Heat," ISIJ International, vol. 50, pp. 1311–1318, Apr. 2010.

[16] O. F. Dilmac and S. K. Ozkan, "Energy and exergy analyses of a steam reforming process for hydrogen production," International Journal of Exergy, vol. 5, no. 2, p. 241, 2008, doi: 10.1504/IJEX.2008.016678.

[17] Z. Wang, J. Mao, Z. He, and F. Liang, "Energy-exergy analysis of an integrated small-scale LT-PEMFC based on steam methane reforming process," Energy Convers Manag, vol. 246, p. 114685, Oct. 2021, doi: 10.1016/j.enconman.2021.114685.

[18] J. Ahn, "Heat Transfer and Thermal Efficiency in Oxy-Fuel Retrofit of 0.5 MW Fire Tube Gas Boiler," Processes, vol. 12, no. 5, p. 959, May 2024, doi: 10.3390/pr12050959.

[19] A. Koopman, A. Rao, B. Marini, C. M. Soares, and D. G. Bogard, "GAS TURBINES IN SIMPLE CYCLE & COMBINED CYCLE APPLICATIONS," National Energy Technology Laboratory .

[20] R. Weber, J. P. Smart, and W. vd Kamp, "On the (MILD) combustion of gaseous, liquid, and solid fuels in high temperature preheated air," Proceedings of the Combustion Institute, vol. 30, no. 2, pp. 2623–2629, Jan. 2005, doi: 10.1016/j.proci.2004.08.101.

[21] C. Robinson and D. B. Smith, "The auto-ignition temperature of methane," J Hazard Mater, vol. 8, no. 3, pp. 199–203, Jan. 1984, doi: 10.1016/0304-3894(84)85001-3.

[22] "Pipeline Basics & Specifics About Natural Gas Pipelines," Sep. 2015. Accessed: Oct. 20, 2024. [Online]. Available: https://pstrust.org/wp-content/uploads/2015/09/2015-PST-Briefing-Paper-02-NatGasBasics.pdf

[23] A. Bejan, G. Tsatsaronis, and M. Moran, "Exergy Analysis," in Thermal Design & Optimization, John Wiley & Son, inc, 1996, ch. 3, pp. 116–117.

[24] M. MORAN, H. SHAPIRO, and D. BOETTNER, "Closed System Exergy Balance," in FUNDAMENTALS OF ENGINEERING THERMODYNAMICS, 8th ed., Wiley, 2014, ch. 7, pp. 379–413.

[25] M. Moran, H. Shapiro, and D. Boettner, "Reacting Mixtures and Combustion," in FUNDAMENTALS OF ENGINEERING THERMODYNAMICS, 8th ed., 2014, ch. 13, pp. 844–854.

[26] I. Dincer and M. A. Rosen, "Chemical exergy," in Exergy, Elsevier, 2021, pp. 37–60. doi: 10.1016/B978-0-12-824372-5.00003-8.

[27] R. Pal, "Chemical exergy of ideal and non-ideal gas mixtures and liquid solutions with applications," International Journal of Mechanical Engineering Education, vol. 47, no. 1, pp. 44–72, Jan. 2019, doi: 10.1177/0306419017749581.

[28] L. Chen, Z. Qi, S. Zhang, J. Su, and G. A. Somorjai, "Catalytic Hydrogen Production from Methane: A Review on Recent Progress and Prospect," Catalysts, vol. 10, no. 8, p. 858, Aug. 2020, doi: 10.3390/catal10080858.

[29] D. Kaya, F. Çanka Kılıç, and H. H. Öztürk, "Energy Efficiency in Boilers," 2021, pp. 265–306. doi: 10.1007/978-3-030-25995-2_9.

[30] "Purchasing Energy-Efficient Large Commercial Boilers," Federal Energy Management Program. Accessed: Oct. 22, 2024. [Online]. Available: https://www.energy.gov/femp/purchasing-energy-efficient-large-commercial-boilers

[31] G. Ludwig, S. Meschkat, and B. Stoffel, "Design Factors Affecting Pump Efficiency," in Energy Efficiency in Motor Driven Systems, Berlin, Heidelberg: Springer Berlin Heidelberg, 2003, pp. 532–538. doi: 10.1007/978-3-642-55475-9_77.

[32] A. Martin-Candilejo, D. Santillán, and L. Garrote, "Pump Efficiency Analysis for Proper Energy Assessment in Optimization of Water Supply Systems," Water (Basel), vol. 12, no. 1, p. 132, Dec. 2019, doi: 10.3390/w12010132.

[33] D. L. Millar, "On the Determination of Efficiency of a Gas Compressor," Energies (Basel), vol. 17, no. 13, p. 3260, Jul. 2024, doi: 10.3390/en17133260.

[34] S. N. Subramanya, V. S. C. Reddy, and V. Madav, "Performance Evaluation of Various Ni-Based Catalysts for the Production of Hydrogen via Steam Methane Reforming Process," in RAiSE-2023, Basel Switzerland: MDPI, Jan. 2024, p. 138. doi: 10.3390/engproc2023059138.

[35] H.-G. Park, S.-Y. Han, K.-W. Jun, Y. Woo, M.-J. Park, and S. K. Kim, "Bench-Scale Steam Reforming of Methane for Hydrogen Production," Catalysts, vol. 9, no. 7, p. 615, Jul. 2019, doi: 10.3390/catal9070615.

[36] "How Gas Turbine Power Plants Work," Office of Fossil Energy and Carbon Management. Accessed: Oct. 26, 2024. [Online]. Available: https://www.energy.gov/fecm/how-gas-turbine-power-plants-work#:~:text=A%20simple%20cycle%20gas%20turbine,of%2060%20percent%20or%20more.

[37] N. Hajjaji, M.-N. Pons, A. Houas, and V. Renaudin, "Exergy analysis: An efficient tool for understanding and improving hydrogen production via the steam methane reforming process," Energy Policy, vol. 42, pp. 392–399, Mar. 2012, doi: 10.1016/j.enpol.2011.12.003.

[38] A. SIMPSON and A. LUTZ, "Exergy analysis of hydrogen production via steam methane reforming," Int J Hydrogen Energy, vol. 32, no. 18, pp. 4811–4820, Dec. 2007, doi: 10.1016/j.ijhydene.2007.08.025.

[39] M. Rosen, "Thermodynamic investigation of hydrogen production by steam-methane reforming," Int J Hydrogen Energy, vol. 16, no. 3, pp. 207–217, 1991, doi: 10.1016/0360-3199(91)90003-2.

[40] J. Lambert, "Analysis of oxygen-enriched combustion for steam methane reforming (SMR)," Energy, vol. 22, no. 8, pp. 817–825, Aug. 1997, doi: 10.1016/S0360-5442(96)00170-3.